Water, heat fluxes and water use efficiency measurement and modeling above a farmland in the North China Plain

QIN Zhong[1], YU Qiang[2], XU Shouhua[2], HU Bingmin[1,3], SUN Xiaomin[2], LIU Enmin[2], WANG Jishun[2], YU Guirui[2] & ZHU Zhilin[2]

1. Ecology academy, College of Life Science, Zhejiang University, Hangzhou 310029,China;
2. Institute of Geographic Sciences and Natural Resources Research, Chinese Academy of Sciences, Beijing 100101, China;
3. College of Science, Zhejiang University, Hangzhou 310029, China
Correspondence should be addressed to Yu Qiang (email: yuq@igsnrr.ac.cn)

Received July 14, 2004; revised January 19, 2005

Abstract Net radiation (R_n), water vapor flux (LE), sensible heat flux (H_s) and soil heat flux (G) were measured above a summer maize field with the eddy-covariance technique, simulation and analysis of water, heat fluxes and crop water use efficiency were made with the RZ-SHAW model at the same time in this study. The results revealed significant diurnal and seasonal variability of water vapor flux for summer maize. Most part of R_n was consumed by the evapotranspiration of the summer maize. The proportion of water vapor flux to net radiation ((LE/R_n) increased with the crop development and peaked around milk-filling stage with a value of 60%, a slightly lower than that obtained by the RZ-SHAW model. Daily evapotranspiration estimated by the model agreed with the results measured with the eddy-covariance technique, indices of agreement (IA) for hourly water vapor fluxes simulated and measured were above 0.75, root mean square errors (RMSE) were no more than 1.0. Diurnal patterns of H_s showed the shape of inverted "U" shifted to the forenoon with a maximum value around 11:30 (Beijing time), while LE exhibited an inverted "V" with a maximum value at around 13:00, about an hour later than H_s. Diurnal change of CO_2 showed an asymmetrical "V" curve and its maximal rates occurred at about 11:30. Variations of water use efficiency during the phonological stages of the summer maize showed a rapid increase with the photosynthetic photon flux density (PPFD) after sunrise, a state of equilibrium around 10:00 followed a decrease. Maximum values of water use efficiency were 24.3, and its average value ranged from 7.6 to 10.3 g kg^{-1}.

Keywords: water vapor flux, CO_2 flux, water use efficiency, RZ-SHAW model, maize, North China Plain.

DOI: 10.1360/05zd0021

It is reported that about 99% of water used in agriculture is lost by crop evapotranspiration (ET) as a vapor form[1]. Quantification of this part of the water loss and the study on the dynamic of soil moisture as well as water and heat transfer on the interface of soil-plant-atmosphere continuum (SPAC) were important for the enhancement of crop field water use efficiency and proper water resources management, especially in the semi-arid region. Measuring directly and estimating with models are two investigation approaches for ET. With the improvement of the instrumentation and the methods of analysis and modeling in the recent time, field experiment integrated together with model simulation, and as a consequence, studies on the crop

evapotranspiration and heat transfer progressed greatly.

Among a set of methods to determine ET directly, the eddy covariance technique has gained predominance recently because of its minimal theoretical assumptions and high accuracy, which allows us to determine the water and carbon fluxes exchange between the atmosphere and the ecosystem biosphere over short time intervals. More often, mass and energy exchange measurements with eddy covariance were used to assess and validate the models[2].

Characteristics and mechanism of the crop evapotranspiration as well as interface water transfer process had been examined and illustrated successfully with the models in the long time development from the single big-leaf models on the basis of Penman-Monteith equation[3,4] to double-layer models derived from the theory of Shuttleworth and Wallace (S-W)[5—7] and even more complex models with multi-layer schemes presented by Oltehev[8], Kustas[9], Kim[10] et al. The USDA-ARS, Root Zone Water Quality Model (RZWQM)[11] and the simultaneous Heat and Water (SHAW) model presented by Flerchinger are two typical models among them[12].

RZWQM, originally established to assume water and solute flow in unsaturated or saturated soil conditions in the crop root has been developed and refined into an integrated physical, biological and chemical process model that simulates plant growth and movement of water, nutrients and pesticides over and through the root zone at a comprehensive area of an agricultural system. Usage of the extended S-W ET model in RZWQM provided the prediction of soil evaporation (bare or residue covered) and canopy transpiration[11]. SHAW is a detailed process model that simulates water and heat movement through a plant-snow-residue-soil system related to soil freezing and thawing as well as computing soil evaporation separately from transpiration abilities[13—16]. Since this model could address soil temperature and water conditions through the winter, incorporation of routines for snow, process of soil heat and soil freezing in the SHAW into the RZWQM might extend applicability of the RZWQM to winter seasons, thus formed the RZ-SHAW model. This coupled model has not been tested except its ability of simulation soil temperature, snow depth and soil frost in winter was reported[17]. The object of this study was to: (1) characterize the water and heat fluxes exchange between the biosphere and atmosphere in summer maize field on the data set obtained in the Yucheng Station, Institute of Geographic Sciences and Natural Resources Research, Chinese Academy of Sciences by the eddy covariance technique and (2) validate RZ-SHAW model in estimating ET and energy fluxes for summer maize field and evaluate model performance with the measurements.

1 Experiment and methods

1.1 Site description

The experiment was performed at Yucheng Comprehensive Experiment Station (36°57′N, 116°36′E, 20 m a.s.l.) in the North China Plain characterized by a semi-humid and monsoon climate. Mean annual precipitation, temperature and global solar radiation at the station over the past 30 years are 528 mm, 13.1℃, and 5225 MJm^{-2} respectively. The underground soils of the area are mainly the moisture soil and the salinized moisture soil. The measurement plot in this study is a winter wheat and summer maize rotation field. Winter wheat is sown in early October and harvested in mid-June while summer maize is sown with the residues of the winter wheat in mid-June and harvested in late September. The terrain surrounding it is vegetated with large, flat areas of crop field, upwind fetch of the site extends more than 5 km for winds from all directions[18].

1.2 Eddy-covariance measurement

Continuous fluxes and meteorological measurements with the eddy covariance technique began on October 20 (day of the year (DOY) 293), 2002. Here only data of summer maize growth stage in 2003 from the day of sowing (June 14, DOY165) to harvest (October 2, DOY275), which accounted to 111 days, were used for this study.

The eddy covariance system, mainly composed

of a 3D sonic anemometer (model CSAT3, Campbell Sci., Logan, UT) and an open path, CO_2/H_2O analyzer (IRGA, Li-7500, Li-Cor Inc., Lincoln, Nebrasks, USA), could measure virtual fluctuations and averages of wind velocity, temperature, water and CO_2 concentrations. Two soil heat flux plates (model HFT-3, Campbell Scientific Inc.) were embedded in between-rows and between-plants to determine fluxes. A data logger (model CR5000, Campbell Sci., Logan, UT) connected with the system operated at 10 Hz and the fluxes were averaged for 30 min periods. Along with the fluxes measurements, standard meteorological data were collected including air pressure, photosynthetic active radiation, net radiation, precipitation, soil temperature, soil moisture, etc.

Leaf area index and height were measured every 5 days. Irrigation and fertilizer were operated to achieve a non-limiting condition throughout the growing season of the summer maize.

1.3 Data processing

Owing to instrument maintenance, calibration, malfunction of the sensors and supporting equipment, missing data in the observed fluxes occupied 5.67% during the period for analysis. Unreasonable data of carbon dioxide flux (F_c), latent heat flux (LE) and sensible heat flux (H_s) rejected accounted for 0.06%, 0.48% and 0.73% respectively after all 30 min raw data were assessed for anomalous turbulent statistics and sensor malfunction[19]. Rejected soil heat fluxes (G) measured between-rows or between-plants comprised 3.06% and 3.41% during the growth period. Major missing fluxes data gap occurred in DOY262-267 because precipitation obscured the gas analyzer optics and sonic transducers. Several strategies were applied to filling these blocks[19—21].

Nighttime fluxes have been reported to be underestimated by the eddy covariance approach during the stable condition because of CO_2 storage in the layer below the eddy flux system. A wind friction velocity (u^*) threshold ($u^* > 0.12$ m s^{-1}) was determined[19,22] and fluxes measurements when u^* was smaller than the threshold were removed from the data set to minimize problems related to insufficient turbulent mixing (fig. 1). In addition, measurements within 24 h after a rain event were eliminated from the data set.

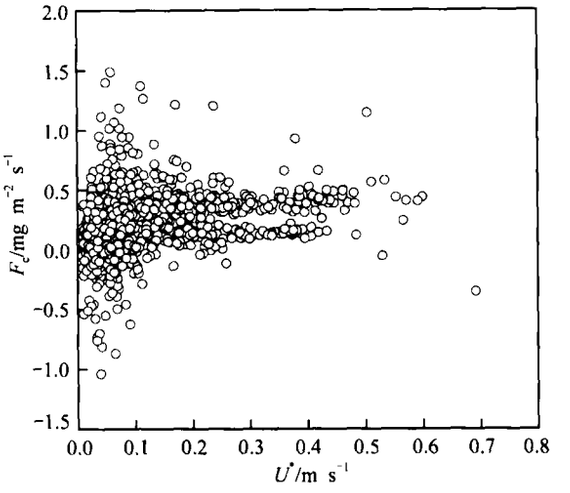

Fig. 1. Measured night F_c (CO_2 flux) vs. nighttime turbulence u^*.

Before gap-filling the missing data, energy closure was examined by the following equation:

$$R_n = G + H_s + LE, \quad (1)$$

where R_n (W m^{-2}), net radiation and G (W m^{-2}), soil heat flux, H_s is the sensible heat flux density (W m^{-2}) on a 30 min basis. Liner regression indicated that agreement between the sum of the turbulent fluxes (LE + H_s) and the available energy (R_a) was generally good (fig. 2):

$$y = 21.745 + 0.806x,\ r^2 = 0.86\ (n = 1951).$$

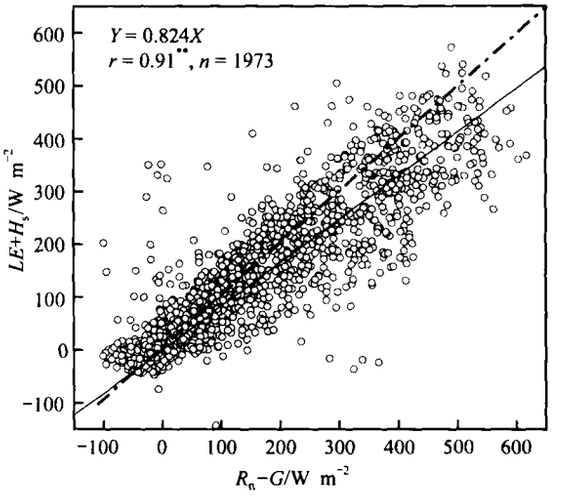

Fig. 2. Half-hourly sums of $LE+H_s$ against available energy (R_n-G) during the summer maize growth.

1.4 Model description

As a modified RZWQM, RZ-SHAW model is a comprehensive model for crop field which consists of several subsystems such as physical, soil chemical, nutrient, pesticide, plant growth processes as well as over-winter process. Among these courses, system *ET* and water and fluxes exchange property above the soil were focused and examined in this paper.

(i) Solar radiation within the canopy. In the layered system of SHAW model, the net radiation absorbed for each layer depends not only on the incoming radiation from above, but on the reflected, scattered and emitted radiation from other layers within the plant canopy, snow, residue, soil system. Therefore the radiation balance was performed by computing the direct, and upward and downward diffuse radiation fluxes above and below each layer.

In RZWQM model[23,24], net radiation over the field reflects the effect of composite albedo on incoming solar radiation and might be approximated by:

$$R_n = [C_c(1-\alpha_c) + C_0C_s(1-\alpha_s) + C_0C_r(1-\alpha_r)]R_s + R_b. \quad (2)$$

where C_c, C_r are the fraction of a unit ground surface area covered by the crop and residue respectively; C_s is the exposed ground area; α_c, α_s, α_r are canopy, soil and residue albedos respectively; R_s is incoming solar shortwave radiation; R_b is net long wave radiation.

(ii) Water and heat transfer within the canopy. Heat flux and temperature within the air space of the canopy in the SHAW model are described by [12, 25]

$$\rho_a C_a \frac{\partial T}{\partial t} = \frac{\partial}{\partial z}\left(\rho_a C_a k_e \frac{\partial T}{\partial z}\right) + H_l, \quad (3)$$

where the terms (W m^{-3}) represent: an energy storage term, which is negligible and not considered in the model; net heat transfer into a layer within a canopy; and a heat source term for heat transfer from the canopy elements (leaves) to the air space within the canopy. In this equation, ρ_a, C_a and T are density (kg m^{-3}), specific heat capacity (J kg^{-1} C^{-1}) and temperature (℃) of the air within the canopy, t is time (s), z is height from the top of the canopy (m), k_e is a transfer coefficient within the canopy (m^2 s^{-1}), and H_l is heat transferred from the vegetation elements (leaves) to the air space within the canopy (W m^{-3}).

Vapor flux through the canopy is written similarly as the heat flux equation:

$$\frac{\partial \rho_v}{\partial t} = \frac{\partial}{\partial z}\left(k_e \frac{\partial \rho_v}{\partial z}\right) + E_l, \quad (4)$$

where the terms (kg s^{-1} m^{-3}) represent: net change in vapor contained within a layer; net vapor flux into a canopy layer; and a source term for transpiration/ evaporation from the canopy elements leaves within the canopy layer. E_l is transpiration or evaporation from the leaves within the canopy and other terms are defined previously.

Transfer of heat and vapor within the canopy is dependent upon location within the canopy, and several approaches for computing the transfer coefficient k_e have been developed. Flerchinger and Pierson[25] used the following expression above the zero plane displacement, d:

$$k_e = k_{u*}(z - d + z_h)/\phi_h, \quad (5)$$

For heights less than d:

$$k_e = k_{u*} z_h / \phi_h, \quad (6)$$

where k is von Karman's constant, u^* is the friction velocity (m s^{-1}), z is height above the residue or soil surface (m), d is the height of the zero plane displacement (m), z_h is the thermal surface roughness parameter (m), and ϕ_h is a diabatic correction factor dependent on the Richardson number computed from H.

Water vapor ($E_{l,i,j}$) and heat transfer ($H_{l,i,j}$) from the vegetation elements (leaves) to the air space within a canopy layer for a given plant species are computed from

$$E_{l,i,j} = L_{ij}\frac{\rho_{vs,i,j} - \rho_{v,i}}{r_{s,i,j} + r_{h,i,j}}, \quad (7)$$

$$H_{l,i,j} = -\rho_a c_a L_{ij}\frac{(T_{l,i,j} - T_i)}{r_{h,i,j}}, \quad (8)$$

where L_{ij} and $T_{l,i,j}$, are leaf area index and leaf temperature of plant species j within canopy layer i, T_i is air temperature within canopy layer i, $\rho_{vs,i,j}$ and $\rho_{v,i}$ are vapor density of plant canopy elements (i.e. leaves) and of air within the canopy, $r_{s,i,j}$ is stomatal resistance per unit of leaf area index and the subscripts refer to plant species j within canopy layer i. $r_{h,i,j}$, the resistance to convective transfer from the canopy leaves per unit leaf area index, is computed from

$$r_{h,i} = 307\left(\frac{d_l}{u_i}\right)^{1/2}. \quad (9)$$

Water flow within the plant is controlled mainly by changes in stomatal resistance. A simple equation relating stomatal resistance to leaf water potential is [26]

$$r_s = r_{so}\left[1+\left(\frac{\psi_l}{\psi_c}\right)^n\right], \quad 10)$$

where d_l is leaf dimension (m), u_i is wind speed within the canopy layer (m s^{-1}), r_{so} is stomatal resistance (m s^{-1}) with no water stress (assumed constant), ψ_c is a critical leaf water potential (m) at which stomatal resistance is twice its minimum value, and n is an empirical coefficient, ψ_l is leaf water potential.

In RZWQM model, the field is divided into two layers, the soil surface and the canopy[11]. The total flux of latent heat above the canopy (i.e., at the measurement height) is written as the sum of latent heat from the canopy and the bare and residue covered soil areas:

$$ET = T + C_s E_s + C_r E_r, \quad (11)$$

where ET, T are evapotranspiration and canopy transpiration rate respectively, C_s and C_r are the fractions of a unit substrate area occupied by bare soil and residue, $C_s+C_r=1$, E_s and E_r are the evaporation per unit area of bare or residue-covered soil respectively.

If the air vapor pressure deficit at the height of the canopy air stream (VPD_0), latent heat from the canopy can be expressed by

$$\lambda T = \frac{\Delta[(R_n - G) - R_{nsub}] + \rho C_p (VPD_0)/r_a^c}{\Delta + \gamma(1 + r_s^c / r_a^c)}, \quad (12)$$

where R_n, R_{nusb} are the flux of net radiation above or below the canopy, G is the heat flux below the canopy(into the substrate), r_a^c is the bulk boundary layer resistance of the canopy elements, r_s^c is the bulk stomatal resistance of the canopy.

$$r_s^c = \frac{r_s}{2LAI_{eff}}, \quad (13)$$

$$r_a^c = \frac{r_b}{2LAI}, \quad (14)$$

where $r_b/2$ is the mean leaf boundary layer resistance of amphistomatous leaves per unit surface area of vegetation.

(iii) Linkage of SHAW with the RZWQM model.

When the routines for over-winter conditions in the SHAW was incorporated into the RZWQM model, expressions for unsaturated hydraulic conductivity, soil matric potential of the RZWQM, the state equation for vertical temperature distribution and water flux in soil from the SHAW, together with an additional equation provided by Fuch's et al.[27] were used to solute problems associated with soil water and heat flux transfer when coupling, this interactions of soil water redistribution routines made it necessary to retain the RZWQM's solution of the Richard's equation within the RZ-SHAW for decoupling the soil heat and water strategies of the SHAW model prior to implementing the energy routines from the SHAW into the RZWQM model. Above the soil surface, the RZ-SHAW routines for heat and water transfer within the canopy, snow and residue layers are solved much the same way as in SHAW model. Detailed numerical solutions were provided by Flerchinger et al.[17]. Once the SHAW model had been coupled with the RZWQM model successfully, routines for net radiation, surface energy balance and transfer were also incorporated into the RZ-SHAW model.

2 Results

2.1 Weather conditions and soil water content

Daily patterns of environmental variables such as air temperature, photosynthetic active radiation, water vapor pressure deficit, precipitation and soil moisture

during the summer maize growth period in 2003 are shown in fig. 3. Average air temperature and photosynthetic active radiation were 25.9℃ and 49.9 MJm^{-2} d^{-1} respectively. The sum of precipitation was 271.1 mm (23.2 mm less than the average value in the past years) for the summer maize growing seasons, occupied about 40.2% of the total amount in the year of 2003. Dynamic of surface soil moisture over the maize growth period was presented in figs. 3(e). There was no water deficit over the maize growth period, soil humidity in the root zone remained 65%—70% of the field water capacity, which allowing for potential evapotranspiration rates (fig. 3(f)).

2.2 Mass and energy transfer over the summer maize field

(i) Diurnal variations of surface fluxes exchange. The mean diurnal cycles of water vapor and heat fluxes as well as CO_2 flux during the maize growth period from jointing to mature stage (DOY201 to DOY202) are shown in fig. 4. Diurnal patterns of H_s showed the shape of inverted "U" shifted to the forenoon with a maximum value around 11:30 (Beijing time), while *LE* exhibited an inverted "V" with a maximum value around 13:00, about an hour later than H_s (fig. 4(a)). Diurnal change of CO_2 showed an asymmetrical "V" curve and the maximal rates of it occurred at about 11:30 (fig. 4(b)).

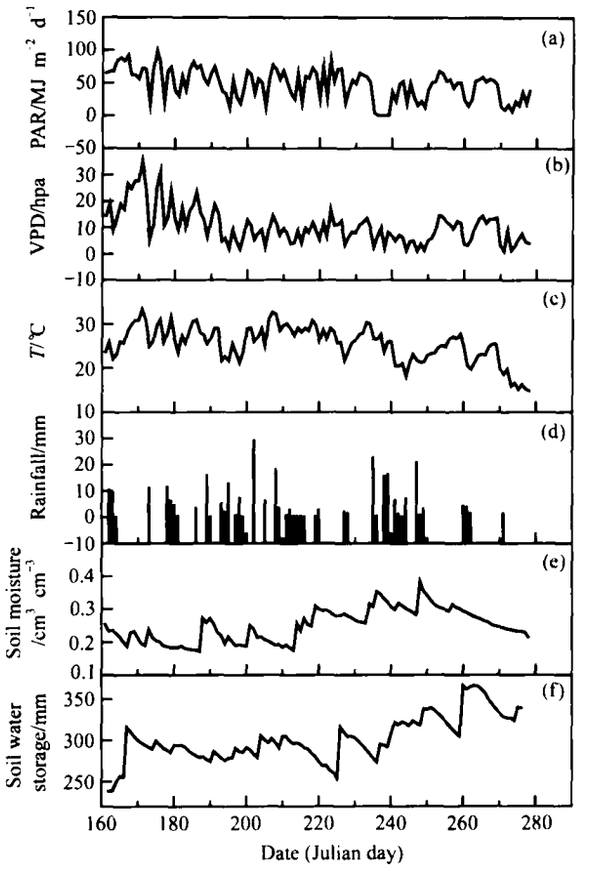

Fig. 3. Daily average photosynthetically active radiation (PAR), water vapor deficit (VPD), air temperature (*T*), 24-h summed rainfall, mean soil volumetric content in 0—5 cm layer and water storage in the root zone (0—40 cm) during the summer maize growth period.

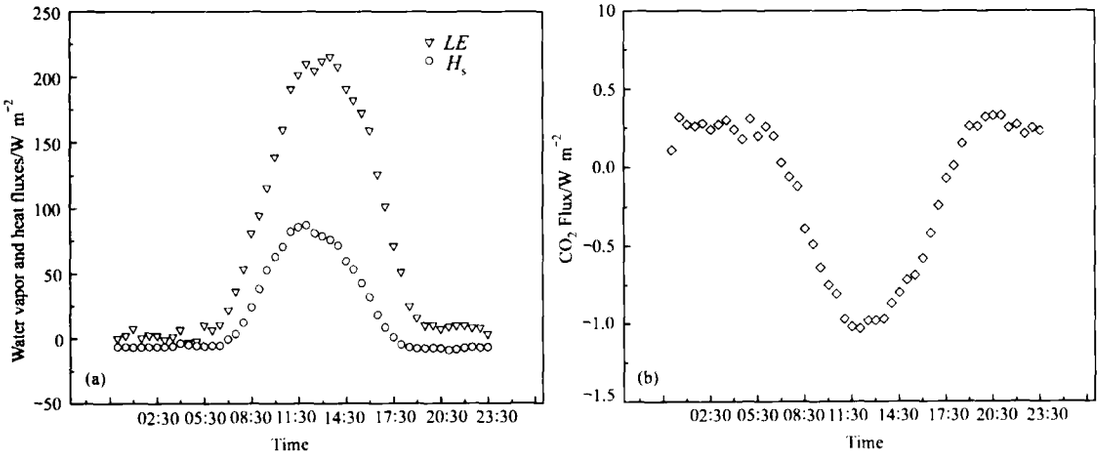

Fig. 4. (a) Diurnal variations of water vapor and heat fluxes; (b) diurnal variation of CO_2 flux.

(ii) Seasonal variations of energy budget components and CO_2 flux. Variations of daytime (07:00—19:00) energy budget components in six phonological stages of the summer maize were examined. Water vapor flux showed a significant seasonal variation (fig. 5). Before leaf emergency, solar radiation went to the soil without the shading effect of the canopy, which led a slight higher of water vapor flux than soil heat flux. After the jointing stage, the canopy developed with the rapid increase of the leaf area, water vapor flux increased greatly while soil heat flux decreased, and the proportion of it to the net radiation (G/R_n) declined from 28.96% in seedling to 7.50% in the mature stage. However, this declined proportion had an increase to 9.05% with leaf senescence in the mature stage, water vapor flux during this period began to decrease. With the sufficient soil water supplement through the growth period of the summer maize, the proportion between the water vapor flux and the net radiation increased with the crop development and maximized during the milk-filling stage with the value of 60%, then decreased moderately in the mature stage. Water vapor flux was a main consumption component of the energy budget (fig. 5).

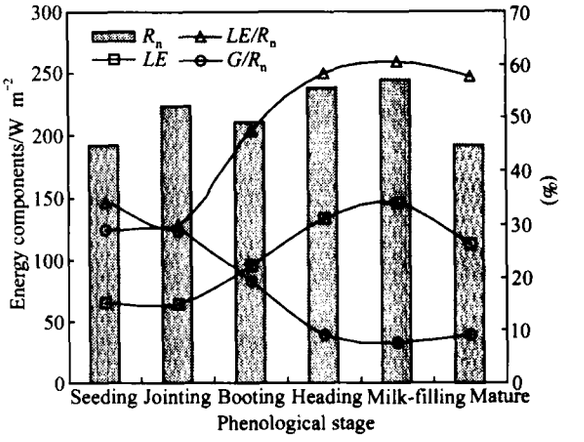

Fig. 5. Energy budget components in the phenological stage.

Variations of the CO_2 flux in the development periods began with jointing are presented in fig. 6. CO_2 flux over the canopy was low with the limited leaf area in the jointing stage of the summer maize, its maximal value was 0.9 mg m^{-2} s^{-1}. With the increasing leaf area, CO_2 flux increased and maximized with a value of 2.0 mg m^{-2} s^{-1} in spin, the peak stage for the growth of the summer maize, then decreased slowly during the mature stage with a value of 1.2 mg m^{-2} s^{-1}.

(iii) Water use efficiency of the summer maize. Half-hourly records of water vapor and CO_2 fluxes in four representative continuous days during the four development stages (jointing, tasseling, milk-filling and mature stages) were selected to determine the water use efficiency in the corresponding period (fig. 7). During the night, when CO_2 flux was positive, indicating that the crop system releases carbon to the atmosphere, water use efficiency was low and negative, and it became near to zero around sunrise or sunset when the photosynthesis and respiration of the maize kept balance. Water use efficiency increased with the photosynthetic photon flux density (PPFD) after sunrise and reached a state of equilibrium at around

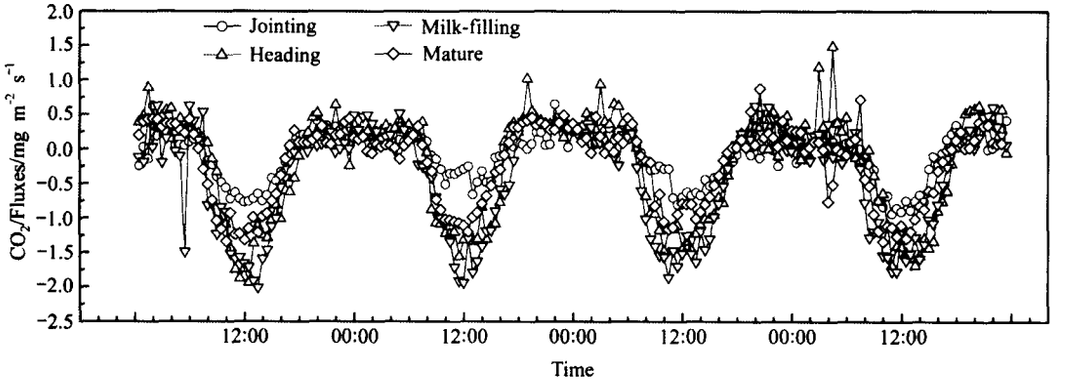

Fig. 6. Variations of CO_2 flux in four phenological stages.

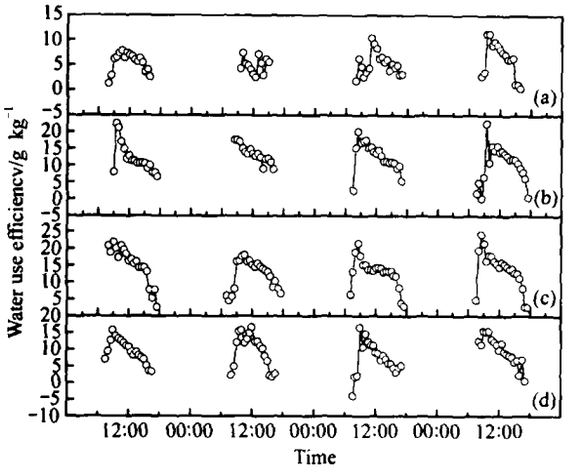

Fig. 7. Water use efficiency in four phonological stages. (a)—(d) represent jointing, heading, milk-filling and mature stages respectively).

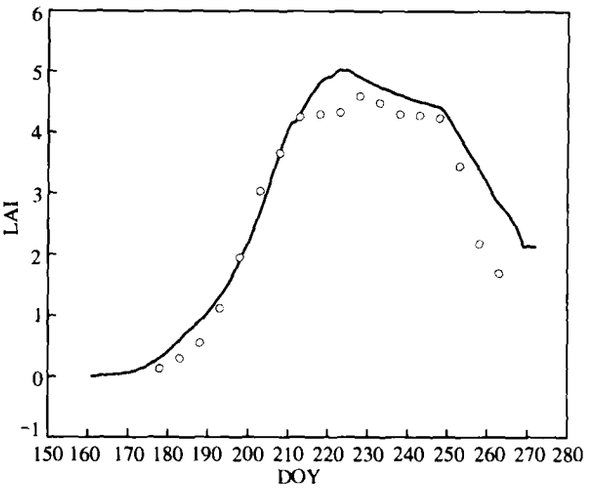

Fig. 8. Measured and simulated evolutions of LAI.

10:00, then decreased after 17:00, average value of water use efficiency ranged 7.6—10.3 g kg^{-1}. After the jointing stage, water use efficiency of the maize increased with the canopy development and maximized in the spin stage of the crop with a value of 24.3 g kg^{-1}, then decreased slowly with the declining photosynthetic ability of the crop community and the concurrent increased respiration consumption in the end of the milk-filling stage. Variations of water use efficiency exhibited the similar pattern with the results in Shijiazhuang, which is located in the same terrain[28].

2.3 Simulation with RZ-SHAW model

(i) Model simulated leaf area index (LAI). LAI has an influence on the surface energy balance and the partition of ET between soil evaporation and crop transpiration. In addition, it is one of most important parameters in the models for the simulation of the crop growth, dynamic of the surface fluxes exchange, etc. Fig. 7 depicts the measured and modeled evolution of LAI throughout the growth period of the summer maize. It showed that the trend of the summer maize growth simulated by RZ-SHAW with daily meteorological data set such as minimum and maximum temperature, wind speed, radiation, and relative humidity from sow to harvest was similar with the measured results with a slightly higher peak values than the latter (fig. 8).

(ii) Dynamic of water vapor flux analysis and simulation. Water vapor flux measured with eddy covariance showed a significant diurnal variation with a pattern of lower values occurring sunrise and sunset while maximum values appeared at around 12:00—14:00. During the entire maize growth period, half-hourly and daily observations of water vapor flux maximized on August 10 (DOY222) when the maize was in its tasseling stage and the potential for evapotranspiration was great. Peak values for them were 486.25 wm^{-2} (0.58 mm H_2O h^{-1}) and 242.52 wm^{-2} (10.2 mm H_2O d^{-1}) respectively. Water vapor flux cumulated for the whole growth courses was 385.3 mm, which is greater than the total precipitation in the same study period (271.1 mm).

Daily ET estimated by the RZ-SHAW model and the measured values through the entire growth period of the summer maize are shown in fig. 9. The square of the linear regression coefficient is 0.83, indicating that the model predicted ET had a good agreement with the values measured with eddy covariance. Total water vapor flux predicted was 396.2 mm, about 2.73% greater than the measured value (fig. 10).

A six-day period from August 17 (DOY235) to August 22 (DOY240), including cloudy days, was selected for the comparison between measured and model-estimated hourly ET values by root mean

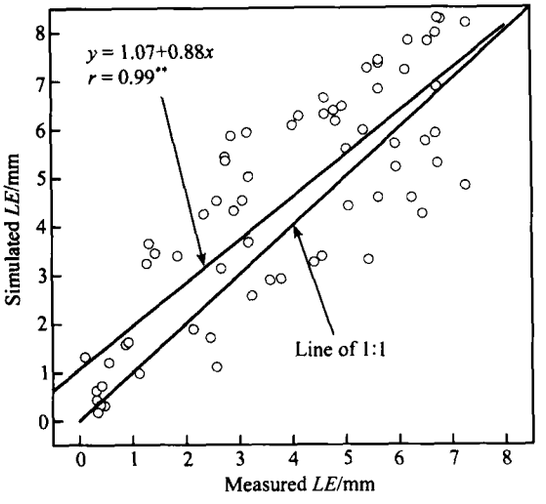

Fig. 9. Daily water vapor flux measured and estimated.

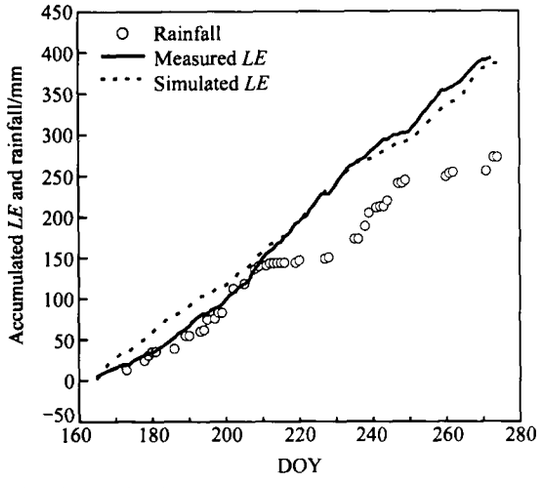

Fig. 10. Accumulated evapotranspiration measured and estimated.

square error (RMSE), systematic mean square error (MSEs) and index of agreement (IA) (table 1).

$$\mathrm{RMSE}=\sqrt{\frac{\sum_{i=1}^{n}(y_i-x_i)^2}{n}}, \tag{15}$$

$$\mathrm{MSEs}=\frac{\sum_{i=1}^{n}(\hat{y}_i-x_i)^2}{n}, \tag{16}$$

$$\mathrm{IA}=1-\frac{\sum_{i=1}^{n}(y_i-x_i)^2}{\sum_{i=1}^{n}[|y_i-\bar{x}|+|x_i-\bar{x}|]^2}, \tag{17}$$

where y_i is the ith observed ET, x_i the ith estimated ET, $\hat{y}_i$ the ith predicted ET through the simple linear regression and $\bar{x}$ is the mean of the estimated values.

All indices of agreement in table 1 were above 0.75 and RMSE were no more than 1.0, indicating that water vapor fluxes estimated by RZ-SHAW were satisfying.

(iii) Variations of energy budget components analysis and prediction. Typical clear sky days in the primary phonological stages were selected to characterize the diurnal variations of energy budget components. Fig. 11 depicts measured and modeled values of energy budget components on June 4 (DOY185), June 29 (DOY210), August 20 (DOY232) and September 16 (DOY259). It showed that the results simulated by RZ-SHAW in four courses had similar trends with that measured by eddy covariance. Diurnal variation of LE coincided with R_n, both of them had a rapid increase after sunrise, peaked at around 12:00—13:00 then decreased. Compared with LE and R_n, H_s and G had lower values and quite smooth variation.

Proportions of LE to R_n (LE/R_n) in the phonological stages estimated by RZ-SHAW were slightly higher than corresponding measured values except the mature stage of the summer maize. This might derive from the diurnal water vapor flux discrepancy observed on the days with high vapor pressure deficit

Table 1 Statistical analysis statistics of measured and simulated water vapor flux

	Aug 17	Aug 18	Aug 19	Aug 20	Aug 21	Aug 22
RMSE	0.85	0.69	0.80	0.74	0.83	0.79
MSEs	32.60	37.30	42.50	40.30	28.70	38.10
IA	0.81	0.77	0.79	0.79	0.85	0.77

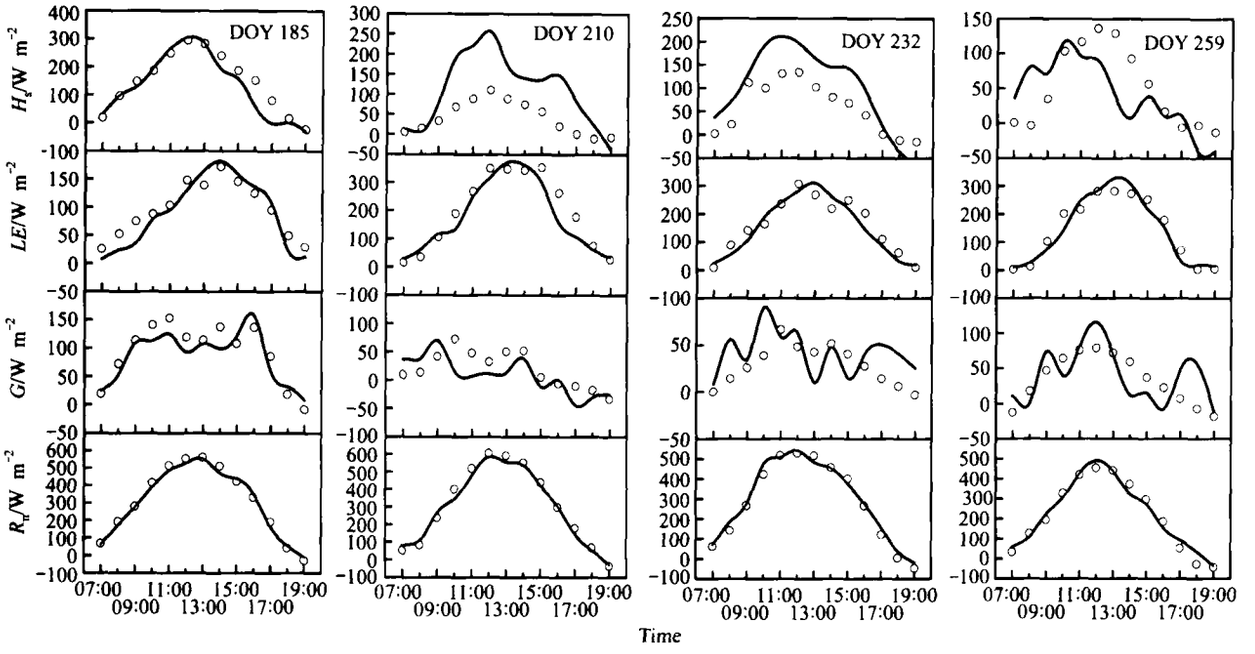

Fig. 11. Daily variations of R_n, G, LE and H_s in selected clear days (circle: measured values; line: simulated values).

and intensive advection, reject of data records within 24 h after the rainfall might impact the results in addition. Maximal LE/R_n and LE/R_a predicted by RZ-SHAW were 65.37% and 70.24 respectively, both occurring in the milk-filling stage, while G/R_n ranged from 6.94% to 22.64%.

3 Conclusions

This paper characterizes variations of energy budget components (R_n, G, LE and H_s) and CO_2 flux measured with the eddy-covariance technique as well as crop water use efficiency, and the results were used to validate the RZ-SHAW model in estimating ET and energy fluxes over a summer maize field. The following contributions have been made:

(1) Diurnal patterns of H_s showed the shape of inverted "U" shifted to the forenoon with a maximum value at around 11:30 (Beijing time), while LE exhibited an inverted "V" with a maximum value at around 13:00, about an hour later than H_s. Diurnal change of CO_2 showed an asymmetrical "V" curve and its maximal rates occurred at about 11:30. Variations of water use efficiency during the phonological stages of the summer maize showed a rapid increase with the photosynthetic photon flux density (PPFD) after sunrise, a state of equilibrium at around 10:00 followed a decrease.

(2) Diurnal variations of energy budget components predicted had the similar trends with the measured results. Proportions of LE/R_n in six phonological stages estimated by RZ-SHAW were slightly higher than the corresponding measured values except the mature stage of the summer maize. Peak values of LE/R_n predicted and measured occurred in the milk-filling stage.

(3) Daily ET predicted by RZ-SHAW had a good agreement with the measured values and the square of the linear regression coefficient is 0.83. Diurnal variation of water vapor flux simulated was in agreement with the measured results. And statistical analysis indicated that the indices of agreement (IA) for hourly water vapor fluxes simulated and measured were above 0.75, the root mean square error (RMSE) was no more than 1.0. These results suggested that the RZ-SHAW model was a useful tool for estimation of evapotranspiration as well as simulation of surface energy transfer.

Acknowledgements The authors would like to thank the Yucheng Station, Institute of Geographic Sciences and Natural Resources Research, Chinese Academy of Sciences for kindly providing data sets. We are indebted to Gerald, N. Flerchinger, Hui Dafeng, Peter Anthoni and Beverly E., Law for their valuable advice and help. The work was supported by the National Science Fund for Overseas Outstanding Youth (Grant No. 40328001) and the Key Research Plan of the Knowledge Innovation Project of the Institute of Geographic Sciences and Natural Resources Research, Chinese Academy of Sciences (Grant No. KZCXI-SW-01).

References

1. Rana, G., Katerji, N., Measurement and estimation of actual evapotranspiration in the field under Mediterranean climate: a review, European Journal of Agronomy, 2000, 13: 125—153.
2. Baldocchi, D. D.,Valentini, R., Oechel, W. et al., Strategies for measuring and modeling carbon dioxide and water vapor fluxes over terrestrial ecosystems. Global Change Biol., 1996, 2: 159—168.
3. Monteith, J. E., Evaporation and Environment, Symp. Soc. Expl. Biol., 1965, 19: 205—234.
4. Noilham. J., Planton, S. A., Simple parameterization of land surface processes for meteorological models, Mon. Wea. Rev., 1989, 117: 536—5493.
5. Deardoff, J. W., Efficient prediction of ground surface temperature and moisture with inclusion of a layer of vegetation, J. Geophys. Res., 1978, 83: 1889—1903
6. Sellers, P. J., Sud, Y. C., Dalcher, A., A simple biosphere model SiB for use within general circulation models, J. Atmos. Sci., 1986, 43: 505—5315.
7. Ace, E., Mihailovic, D. T., A coupled soil moisture and surface temperature prediction model, J. Appl. Meteor., 1991, 30: 812—822.
8. Oltechev, A., Constantin, J., Gravenhorst, G. et al., Application of a six-layer SVAT model from simulation of evapotranspiration and water uptake in a sparse forest, Physics and Chemistry of the Earth, 1996, 21(3): 195—199.
9. Kustas, W. P., On using mixed-layer transport parameterizations with radiometric surface temperature for computing regional scale sensible heat flux, Boundary-layer Meteorol., 1996, 80(3): 205—211.
10. Kim, C. P., Impact of soil heterogeneity in a mixed-layer model of the planetary boundary layer, Hydrological Sciences Journal, 1998, 43(4): 633—658.
11. USDA-ARS, Root zone water quality model, RZWQM98, GPSR Technical Report No. 3. USDA-ARS Great Plains Systems Research Unit, Ft. Collins, CO., 1998.
12. Flerchinger, G. N., Hanson, C. L., Wight, J. R., Modeling of evapotranspiration and surface energy budgets across awatershed, Water Resour. Res., 1996, 32(8): 2539—2548.
13. Flerchinger, G. N., Cooley, K. R., Deng, Y., Impacts of spatially and temporally varying snowmelt on subsurface flow in a mountainous watershed, 1. Snowmelt simulation, Hydrol. Sci. J., 1994, 39: 507—520.
14. Flerchinger, G. N., Cooley, K. R., Hanson, C. L. et al., A uniform versus an aggregated water balance of a semi-arid watershed, Hydrol. Proc., 1998a, 12: 331—342.
15. Flerchinger, G. N., Hanson, C. L., Wight, J. R., Modeling of evapotranspiration and surface energy budgets across a watershed, Water Resour. Res., 1996b, 32(8): 2539—2548.
16. Flerchinger, G. N., Kustas, W. P., Weltz, M. A., Simulating surface energy fluxes and radiometric surface temperatures for two arid vegetation communities using the SHAW model, J. Appl. Meteorol., 1998b, 37(5): 449—460.
17. Flerchinger, G. N., Aiken, R. M., Rojas, K. W. et al., Development of the root zone water quality model (RZWQM) for over-winter conditions, American Society of Agricultural Engineers, 1999, 43(1): 59—68.
18. Lee, X. H., Yu Q., Sun X. M. et al., Micrometeorological fluxes under the influence of regional and local advection: a revisit. Agricultural and Forest Meteorology, 2004, 122: 111—124
19. Falge, E., Baldocchi, D., Olson, R., Gap filling strategies for defensible annual sums of net ecosystem exchange, Agri. Forest Meteorol., 2001, 107: 43—69
20. Black, T. A., Ethier, G. J., Dewitt, G. B., Annual and seasonal variability of sensible and latent heat fluxes above a coastal Douglas-fir forest, British Columbia, Canada. E. R. Humphreys. Agri. Forest Meteorol., 2003, 115: 109—125.
21. Kell, B., Wilson, D., Baldocchi, D., Seasonal and interannual variability of energy fluxes over a broadleaved temperate deciduous forest in North America, Agri. Forest Meteorol., 2000, 100: 1—18.
22. Anthoni, P. M., Annette, F., Olaf, K. et al., Winter wheat carbon exchange in Thuringia, Germany, Agricultural and Forest Meteorology, 2004, 121: 55—67.
23. Snane, M. H., Gregoryanf, J. M., McCarty, T. R., Water use prediction for residue management systems, ASAE. St. Joseph, MI. Paper, 1984, No. 84—2016.
24. DeCoursey, D. G., Evaporation and transpiration processes, In Root Zone Water Quality Model (version 1.0), Technical Documentation. Fort Collins, CO., 1992, 29—74.
25. Flerchinger, G. N., Pierson, F. B., Modeling plant canopy effects on variability of soil temperature and water, Agric. and Forest Meteor., 1991, 56: 227—246.
26. Campbell, G. S., Soil Physics with BASIC: Transport Models for Soil-plant Systems, Amsterdam: Elsevier, 1985, 150.
27. Fuchs, M., Campbell, G. S., Papendick, R. I., An analysis of sensible and latent heat flow in a partially frozen unsaturated soil, Soil Sci. Soc. Am. J., 1978, 42(3): 379—385.
28. Zhang, Y. Q., Shen Y. J., Liu, C. M. et al., Measurement and Analysis of water, heat and CO_2 flux from a farmland in the North China Plain, Acta Geographical Sinica (in Chinese), 2002, 57: 333—342.